J Braz. Soc. Mech. Sci. Eng. (2017) 39:969–980
DOI 10.1007/s40430-016-0555-1

TECHNICAL PAPER

Thermally induced buckling of thin annular FGM plates

M. Yousefitabar[1] · M. Kh. Matapouri[1]

Received: 24 February 2015 / Accepted: 26 April 2016 / Published online: 13 May 2016

Abstract This article discusses the instability of thin annular FG plates subjected to transversely distributed temperature loading. Based on the classical thin plate theory, equilibrium equations of an annular FG plate are obtained. Plate is assumed to be graded in the thickness direction whose material properties vary smoothly according to the power law form. Existence of bifurcation buckling for various boundary conditions are examined and stability equations are obtained by means of the adjacent equilibrium criterion. An analytical solution is presented to calculate the thermal buckling load by finding the exact eigenvalues of the stability equation. Three types of thermal loading, namely uniform temperature rise, transversely linear temperature and heat conduction across the thickness are studied. The effects of thickness, power law index and thermal loading type on the critical buckling temperature of FG plates are presented comprehensively. It is found that, while the temperature loading through the plate is symmetric, first buckled configuration of a fully clamped FGM plate is always asymmetric.

Keywords Buckling · Functionally graded material · Annular plate · Classical plate theory

Technical Editor: Fernando Alves Rochinha.

✉ M. Kh. Matapouri
mkhmata@gmail.com

[1] Department of Mechanical Engineering, Islamic Azad University, South Tehran Branch, Tehran, Iran

1 Introduction

Functionally graded materials are one of the novel class of materials whose thermo-mechanical properties vary smoothly in one or more directions based on a position-dependent function. Analysis of solid structures such as beams, plates and shells made of FGMs have attracted increasing attention due to the interesting behaviour of FG solids. A number of wealth investigations are observed through the open literature on static and dynamic analysis of circular, annular and sectorial plates. Among them, Nie and Zhong [1] developed a semi-analytical approach to treat the symmetrical bending of functionally graded annular and circular plates. Two directional FG plates whose properties vary continuously according to an exponential function in radial and thickness directions are assumed in their work. After presenting two coupled elasticity equations, a state space method in thickness direction combined with DQM technique along radial axis is used to discrete the governing equations. A modification of [1] is reported in [2] to the free vibration problem of annular plates including multi-directional non-homogeneity. First-order theory-based formulation to analyse the non-linear symmetric and asymmetric behaviour of circular FG plates is reported by Noseir and Fallah [3]. A perturbation solution in conjunction with circumferential Fourier expansion is developed to overcome the highly non-linear equilibrium equations. Reddy et al. [4] presented explicit closed-form expressions to study both thin and moderately thick annular and circular FG plates subjected to axisymmetric loading. Axisymmetric bending of thick functionally graded circular plates based on a third-order shear deformation plate theory is reported by Saidi et al. [5]. Their study covers various types of boundary conditions for outer edge of the plate and closed-form expressions are obtained for stress,

deflection and moment distribution through the plate. Sahraee and Saidi [6] examined the bending and stretching of thick FG plates subjected to uniform transverse mechanical loading. Based on a fourth-order shear deformable plates theory, four coupled ordinary differential equations are established. For the case when properties are graded across the thickness, stretching–bending coupling exists through the formulation. Noseir and Fallah [7] proposed a reformulation for FGM plates in polar coordinates in which five highly coupled equilibrium equations are decoupled and represented in terms on two new PDEs known as edge zone and interior zone functions. Free vibration of annular FG plates based on the moderately thick plate theory is done by Hosseini Hashemi et al. [8]. After deriving five highly coupled partially differential equations, and employing the decoupling method proposed by Noseir an Fallah [7], closed-form explicit expressions to cover the natural frequencies of various types of FG plates covering possible combinations of free, clamped, soft and hard simply supported edges for inner and outer boundaries of the plate are presented. Assuming exponentially distributed mechanical properties for FG plates, Dong [9] investigated three-dimensional free vibration of annular FG plates via a Ritz method, where displacements are chosen as a proper sets of Chebyshev polynomials. Aghdam et al. [10] investigated the implementation of Extended Kantorovich Method (EKM) in static analysis of sectorial FG plates. Their study is limited to fully clamped plates subjected to uniformly distributed lateral mechanical loading. A polynomial Ritz-based eigenvalue analysis is performed by Tajeddini et al. [11] to study the vibration problem of annular and circular plates made of FGMs. A finite elements-based formulation is developed by Afsar and Go [12] to analyse the thermoelastic bending response of rotating FGM annular disks with radial heterogeneity.

Prediction of the bifurcation point of the solid structures subjected to in-plane mechanical or thermal loading is one of the most important factors in design. Growth of FG structures, and especially circular, annular or sectorial FG plates, have necessitated more investigation on this subject to reach a reliable design. Among the primary works on this subject, Najafizadeh and Eslami performed the buckling of thin solid circular plates made of FGMs subjected to mechanical [13] and thermal [14] loading. Their investigations are limited to the symmetrical buckling. Following Kirchhoff plate theory of thin structures, the equilibrium and stability equations in general form are obtained and eigenvalue solution of stability equations is done and closed-form phrases are reported to predict the bifurcation-point temperatures or loads of thin circular FG plates. When mechanical properties of FG plates are graded across the thickness of the plate according to power law form, Najafizadeh and Heydari [15, 16] treated the thermal and mechanical buckling load of thick FG plates based on the von-Karman non-linearity and Reddy's third-order thick plate theory. Reliable explicit expressions are resulted in their work. A pseudo-spectral method to solve the thermally induced buckling problem of circular FG plates with variable thickness is done by Jalali et al. [17]. Based on the first-order theory of laminated plates, stability equations are solved via the Chebyshev polynomials. Ma and Wang [18] did the post-buckling and non-linear bending of circular FG plate when loading cases are symmetric. A numerical shooting method is adopted to solve the non-linear coupled ordinary differential equations. To compare the influences of three available homogenization schemes on critical buckling temperature and heat flux and also post-buckling equilibrium path of FGM solid circular plates, a Ritz-based formulation with polynomial shape functions is used by Kiani and Eslami [19]. Mechanical buckling, thermal buckling, and elastic foundation effect of mechanical buckling of sectorial plates are reported by Saidi and co-authors [20–22]. All of these works are formulated based on the first-order plate theory and five partially differential equations are established as stability equations. After decoupling equations, Levy-type solution of plates is adopted to solve the instability problem of sectorial FG plates under various boundary conditions. However, pre-buckling analysis of a plate is not well executed in [21], where the problem is posed as a primary–secondary equilibrium configuration instead of the non-linear bending. Also Li et al. [23] presented the non-linear bending and post-buckling of heated elastic FG circular plates for imperfect and perfect plates based on a shooting method. Recently, Kiani and Eslami [24, 25] discussed the thermal bifurcation and buckled configurations of an FGM circular/annular plate resting over elastic foundation. It has been shown that the fundamental buckled shape of an annular plate over a complete elastic foundation, or a circular plate over a partial/complete elastic foundation may be asymmetric. Sepahi et al. [26] adopted the GDQ method to solve the non-linear equilibrium equations of radially graded FGM annular plate. A shooting method is adopted in [27] by Aghelinejad et al. to obtain the critical buckling temperature and post-buckling equilibrium path of transversely graded annular FG plate. Reported works of [26, 27] consider only the symmetrical shape for buckling state and post-buckling regime of the clamped annular FGM plates.

Various analytical eigenvalue analysis are reported for instability of FGM circular plates. There is, however, no analytical work covering the elastic instability of heated annular FG plates in asymmetrical shape using a single transcendental equation. Examination of the existence of asymmetrical buckling modes at the presence of symmetrical loadings and revealing the real state of the plate under the in-plane thermal loads are the main factors that

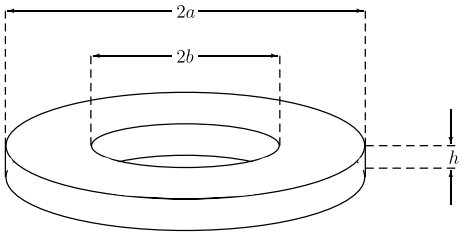

Fig. 1 Geometry of a thin annular FGM plate

are discussed in this research. Based on the classical theory of plates and the von-Karman non-linearity in polar coordinate, equilibrium equations of an annular plate are derived. Pre-buckling analysis of the plate with the assumption of immovable edges is executed and proper boundary conditions are chosen to assure the existence of bifurcation-type buckling. Stability equations of the plate are derived in general form and asymmetrical eigenvalue solution is performed. In each case of thermal loading, closed-form expressions are presented to estimate the critical buckling temperatures as well as the buckled shapes. Results show that the number of nodal diameters of clamped annular FG plates are identical with those of obtained for isotropic homogeneous plates.

2 Governing equations

Consider an annular plate made of FGMs of thickness h, inner radii b, and outer radii a, referred to the polar coordinates (r, θ, z), as shown in Fig. 1. As a rule of thermo-mechanical property distribution, a power law form is chosen which dictates the dispersion of ceramic volume fraction V_c and metal volume fraction V_m as follows:

$$V_c = \left(\frac{1}{2} + \frac{z}{h}\right)^k, \quad V_m = 1 - V_c \tag{1}$$

Shen and Wang [28] made a comparison on the Voigt rule of mixture and Mori-Tanaka scheme for the non-linear vibration problem of rectangular FGM plates. It is shown that the difference between these two methods is negligible. Therefore, in this study the simple scheme of Voigt rule of mixture is used. Based on the Voigt rule [13, 14], thermo-mechanical properties of the FGM plate, may be expressed as the linear function of each property and volume fractions. By means of this rule and Eq. (1), a non-homogeneous property of the plate, P, as a function of thickness direction may be written as

$$P(z) = P_m + P_{cm}\left(\frac{1}{2} + \frac{z}{h}\right)^k, \quad P_{cm} = P_c - P_m \tag{2}$$

where P_m and P_c are the corresponding properties of the metal and ceramic, respectively, and k is a non-negative constant called the power law index and shows the sharpness of property dispersion. In the present work, we assume that modulus of elasticity, E, thermal conductivity, K, and the thermal expansion coefficient, α, are described by Eq. (2), while Poisson's ratio, ν, is considered to be constant across the thickness [20–22]. This assumption has been established in a large number of studies, since Poisson's ratio generally varies in a small range.

The von-Karman-type non-linear strain-displacement relations in polar coordinate, considering the thin plate theory assumptions, are [13, 14]

$$\begin{aligned}
\varepsilon_{rr} &= u_{,r} + \frac{1}{2}w_{,r}^2 \\
\varepsilon_{\theta\theta} &= \frac{1}{r}v_{,\theta} + \frac{1}{r}u + \frac{1}{2r^2}w_{,\theta}^2 \\
\gamma_{r\theta} &= \frac{1}{r}u_{,\theta} + v_{,r} - \frac{1}{r}v + \frac{1}{r}w_{,\theta}w_{,r}
\end{aligned} \tag{3}$$

Here, ε_{rr} and $\varepsilon_{\theta\theta}$ are the normal strains and $\gamma_{r\theta}$ is the shear strain, and a comma indicates partial derivative. Besides, u, v and w are the radial, circumferential and lateral displacements, respectively.

In this study, the classical plate theory with Kirchhoff assumptions is used with the following displacement field [13, 14]

$$\begin{aligned}
u(r,\theta,z) &= u_0(r,\theta) - zw_{0,r}(r,\theta) \\
v(r,\theta,z) &= v_0(r,\theta) - \frac{z}{r}w_{0,\theta}(r,\theta) \\
w(r,\theta,z) &= w_0(r,\theta)
\end{aligned} \tag{4}$$

where u_0, v_0, and w_0 represent the displacements of the mid-surface $(z = 0)$ along r, θ, and z directions, respectively.

Considering T and T_0 as temperature distribution and reference temperature, respectively, the constitutive law for the FGM plate subjected to thermal loadings becomes [29]

$$\begin{Bmatrix} \sigma_{rr} \\ \sigma_{\theta\theta} \\ \tau_{r\theta} \end{Bmatrix} = \frac{E}{1-\nu^2}\begin{bmatrix} 1 & \nu & 0 \\ \nu & 1 & 0 \\ 0 & 0 & \frac{1-\nu}{2} \end{bmatrix}\left(\begin{Bmatrix} \varepsilon_{rr} \\ \varepsilon_{\theta\theta} \\ \gamma_{r\theta} \end{Bmatrix} - (T - T_0)\begin{Bmatrix} \alpha \\ \alpha \\ 0 \end{Bmatrix}\right) \tag{5}$$

Based on the classical plate theory, the stress resultants are related to the stresses through the following equations [13]

$$\begin{aligned}
(N_{rr}, N_{\theta\theta}, N_{r\theta}) &= \int_{-\frac{h}{2}}^{\frac{h}{2}} (\sigma_{rr}, \sigma_{\theta\theta}, \tau_{r\theta})\mathrm{d}z \\
(M_{rr}, M_{\theta\theta}, M_{r\theta}) &= \int_{-\frac{h}{2}}^{\frac{h}{2}} z(\sigma_{rr}, \sigma_{\theta\theta}, \tau_{r\theta})\mathrm{d}z
\end{aligned} \tag{6}$$

Substituting Eqs. (3), (4), and (5) into (6) gives the stress resultants in terms of the mid-plane displacement as

$$\begin{Bmatrix} N_{rr} \\ N_{\theta\theta} \\ N_{r\theta} \\ M_{rr} \\ M_{\theta\theta} \\ M_{r\theta} \end{Bmatrix} = \frac{1}{1-\nu^2} \times \begin{bmatrix} E_1 & \nu E_1 & 0 & E_2 & \nu E_2 & 0 \\ \nu E_1 & E_1 & 0 & \nu E_2 & E_2 & 0 \\ 0 & 0 & \frac{1-\nu}{2}E_1 & 0 & 0 & \frac{1-\nu}{2}E_2 \\ E_2 & \nu E_2 & 0 & E_3 & \nu E_3 & 0 \\ \nu E_2 & E_2 & 0 & \nu E_3 & E_3 & 0 \\ 0 & 0 & \frac{1-\nu}{2}E_2 & 0 & 0 & \frac{1-\nu}{2}E_3 \end{bmatrix}$$

$$\begin{Bmatrix} u_{0,r} + \frac{1}{2}w_{0,r}^2 \\ \frac{1}{r}v_{0,\theta} + \frac{1}{r}u_0 + \frac{1}{2r^2}w_{0,\theta}^2 \\ \frac{1}{r}u_{0,\theta} + v_{0,r} - \frac{1}{r}v_0 + \frac{1}{r}w_{0,r}w_{0,\theta} \\ -w_{0,rr} \\ -\frac{1}{r^2}w_{0,\theta\theta} - \frac{1}{r}w_{0,r} \\ -\frac{2}{r}w_{0,r\theta} + \frac{2}{r^2}w_{0,\theta} \end{Bmatrix} - \begin{Bmatrix} N^T \\ N^T \\ 0 \\ M^T \\ M^T \\ 0 \end{Bmatrix} \tag{7}$$

where N^T and M^T are the thermal force and thermal moment resultants and E_1, E_2, and E_3 are constants to be calculated as

$$E_1 = \int_{-\frac{h}{2}}^{\frac{h}{2}} E(z)\mathrm{d}z = h\left(E_m + \frac{E_{cm}}{k+1}\right) = he_1$$

$$E_2 = \int_{-\frac{h}{2}}^{\frac{h}{2}} zE(z)\mathrm{d}z = h^2E_{cm}\left(\frac{1}{k+2} - \frac{1}{2k+2}\right) = h^2e_2$$

$$E_3 = \int_{-\frac{h}{2}}^{\frac{h}{2}} z^2E(z)\mathrm{d}z = h^3\left(\frac{1}{12}E_m + E_{cm}\left(\frac{1}{k+3} - \frac{1}{k+2} + \frac{1}{4k+4}\right)\right) = h^3e_3$$

$$N^T = \frac{1}{1-\nu}\int_{-\frac{h}{2}}^{\frac{h}{2}} E(z)\alpha(z)(T-T_0)\mathrm{d}z$$

$$M^T = \frac{1}{1-\nu}\int_{-\frac{h}{2}}^{\frac{h}{2}} zE(z)\alpha(z)(T-T_0)\mathrm{d}z \tag{8}$$

The equilibrium equations of an annular FGM plate under thermal loadings may be derived on the basis of the stationary potential energy. The total virtual potential energy of the plate, δU, is equal to the total virtual strain energy of the plate, that is,

$$\delta U = \int_b^a \int_0^{2\pi} \int_{-\frac{h}{2}}^{\frac{h}{2}} (\sigma_{rr}\delta\varepsilon_{rr} + \sigma_{\theta\theta}\delta\varepsilon_{\theta\theta} + \tau_{r\theta}\delta\gamma_{r\theta})r\mathrm{d}z\mathrm{d}\theta\mathrm{d}r \tag{9}$$

Using Eqs. (7) and (8) and employing the virtual work principle to minimize the functional of total potential energy function and performing some proper mathematical simplifications yield the expressions for the equilibrium equations of FGM plate as below

$$\delta u_0 : N_{rr,r} + \frac{1}{r}N_{r\theta,\theta} + \frac{1}{r}(N_{rr} - N_{\theta\theta}) = 0$$

$$\delta v_0 : N_{r\theta,r} + \frac{2}{r}N_{r\theta} + \frac{1}{r}N_{\theta\theta,\theta} = 0$$

$$\begin{aligned} \delta w_0 : {} & M_{rr,rr} + \frac{2}{r}M_{rr,r} + \frac{1}{r^2}M_{\theta\theta,\theta\theta} - \frac{1}{r}M_{\theta\theta,r} + \frac{2}{r}M_{r\theta,r\theta} \\ & + \frac{2}{r^2}M_{r\theta,\theta} + N_{rr}w_{0,rr} + N_{\theta\theta}\left(\frac{1}{r^2}w_{0,\theta\theta} + \frac{1}{r}w_{0,r}\right) \\ & + 2N_{r\theta}\left(\frac{1}{r}w_{0,r\theta} - \frac{1}{r^2}w_{0,\theta}\right) = 0 \end{aligned} \tag{10}$$

3 Existence of bifurcation-type buckling

In the previous section, the equilibrium equations are derived for an annular FGM plate. To obtain the in-plane loads, pre-buckling analysis should be done. When a bifurcation point exists in load-deflection path of the plate, a pre-buckling configuration is revealed when the non-linear terms are omitted from Eq. (7). Consider an FGM plate that is subjected to transverse symmetrical temperature loading case.

Assume that the FGM plate exhibits a bifurcation-type buckling. Therefore, prior to buckling, plate experiences an in-plane regime of displacements. Neglecting the lateral deflection of the plate in pre-buckling state (since bifurcation exists, plate does not experience any lateral deflection) and solving the symmetrical type of the equilibrium equations in conjunction with the immovability conditions on inner and outer edges, yields

$$u_0^0(r,\theta) = 0 \tag{11}$$

Here, a superscript 0, indicates the pre-buckling conditions.

Now, by means of Eq. (7) and neglecting the lateral deflection of the plate in pre-buckling state, the following pre-buckling forces are obtained

$$N_{rr}^0 = N_{\theta\theta}^0 = -N^T,\ N_{r\theta}^0 = 0 \tag{12}$$

While the in-plane resultants are obtained, extra pre-buckling moments exist which are equal to

$$M^0_{rr} = M^0_{\theta\theta} = -M^T,\ M^0_{r\theta} = 0 \tag{13}$$

These thermal moments, in general, are not zero due to the mid-plane asymmetric configuration of FG annular plates. The existence of thermal moments in pre-buckling state means that, plate bends at the onset of thermal loading. Only in a special case, extra moments vanish through the plate and that is when edges are capable of supplying moments. Among three types of boundary conditions (Free, Clamped and Simply supported) only clamped edges are capable of handling extra moments. This phenomenon arises from the fact that kinematic boundary conditions of clamping are not affected by temperature distribution. Therefore, only annular plates which are clamped at inner and outer edges show a bifurcation-type buckling under thermal loading, and only this type is considered in this paper. This conclusion is compatible with the findings of other researchers for flat beams and plates of various shapes, see e.g. [30–43]. Note that, for annular plate with both boundaries clamped, based to the Eq. (11), in pre-buckling state, all three components of displacement field are equal to zero.

4 Stability equations

The stability equations of an FG annular plate may be obtained by means of the adjacent equilibrium criterion [15, 16]. Let us assume that the state of equilibrium of FGM plate under loads is defined in terms of the displacement components u^0_0, v^0_0, and w^0_0. The displacement components of a neighbouring state of the stable equilibrium differ by u^1_0, v^1_0, and w^1_0 with respect to the equilibrium position. Thus, the total displacements of a neighbouring state are [15, 16]

$$u_0 = u^0_0 + u^1_0, \quad v_0 = v^0_0 + v^1_0, \quad w_0 = w^0_0 + w^1_0 \tag{14}$$

Accordingly, the stress resultants are divided into two terms representing the stable equilibrium and the adjacent state. The stress resultants with superscript 1 are linear functions of displacement with superscript 1. Considering this and using Eqs. (7) and (10), and performing proper simplifications, the stability equations become

$$N^1_{rr,r} + \frac{1}{r}N^1_{r\theta,\theta} + \frac{1}{r}(N^1_{rr} - N^1_{\theta\theta}) = 0$$

$$N^1_{r\theta,r} + \frac{2}{r}N^1_{r\theta} + \frac{1}{r}N^1_{\theta,\theta} = 0$$

$$\begin{aligned} &M^1_{rr,rr} + \frac{2}{r}M^1_{rr,r} + \frac{1}{r^2}M^1_{\theta\theta,\theta\theta} - \frac{1}{r}M^1_{\theta\theta,\theta} \\ &\quad + \frac{2}{r}M^1_{r\theta,r\theta} + \frac{2}{r^2}M^1_{r\theta,\theta} \\ &\quad + N^0_{rr}w^1_{0,rr} + N^0_{\theta\theta}\left(\frac{1}{r^2}w^1_{0,\theta\theta} + \frac{1}{r}w^1_{0,r}\right) \\ &\quad + 2N^0_{r\theta}\left(\frac{1}{r}w^1_{0,r\theta} - \frac{1}{r^2}w^1_{0,\theta}\right) = 0 \end{aligned} \tag{15}$$

The stability equations in terms of the displacement components may be obtained by substituting Eq. (7) into the above equations. Upon substitution, second and higher order terms of the incremental displacements may be omitted [14, 16]. Resulting equations are three stability equations based on the classical plate theory for an FGM plate

$$\begin{aligned} &E_1\left(u^1_{0,rr} + \frac{1}{r}u^1_{0,r} - \frac{1}{r^2}u^1_0 - \frac{1}{r^2}v^1_{0,\theta} + \frac{1}{r}v^1_{0,r\theta}\right) \\ &\quad + \frac{(1-\nu)}{2}E_1\left(\frac{1}{r^2}u^1_{0,\theta\theta} - \frac{1}{r}v^1_{0,r\theta} - \frac{1}{r^2}v^1_{0,\theta}\right) \\ &\quad - E_2\left(w^1_{0,rrr} - \frac{1}{r^2}w^1_{0,r} + \frac{1}{r}w^1_{0,rr} - \frac{2}{r^3}w^1_{0,\theta\theta} + \frac{1}{r^2}w^1_{0,\theta\theta r}\right) = 0 \end{aligned}$$

$$\begin{aligned} &E_1\left(\frac{1}{r^2}v^1_{0,\theta\theta} + \frac{1}{r}u^1_{0,r\theta} + \frac{1}{r^2}u^1_{0,\theta}\right) \\ &\quad + \frac{(1-\nu)}{2}E_1\left(v^1_{0,rr} + \frac{1}{r}v^1_{0,r} - \frac{1}{r^2}v^1_0 + \frac{1}{r^2}u^1_{0,\theta} - \frac{1}{r}u^1_{0,r\theta}\right) \\ &\quad - E_2\left(\frac{1}{r}w^1_{0,rr\theta} + \frac{1}{r^2}w^1_{0,r\theta} + \frac{1}{r^3}w^1_{0,\theta\theta\theta}\right) = 0 \end{aligned}$$

$$\begin{aligned} &\frac{E_2}{1-\nu^2}\left(u^1_{0,rrr} + \frac{2}{r}u^1_{0,rr} - \frac{1}{r^2}u^1_{0,r} + \frac{1}{r^3}u^1_0 + \frac{1}{r^3}u^1_{0,\theta\theta} + \frac{1}{r^2}u^1_{0,r\theta\theta} - \frac{1}{r^2}v^1_{0,r\theta} + \frac{1}{r^3}v^1_{0,\theta} + \frac{1}{r^3}v^1_{0,\theta\theta\theta}\right. \\ &\left. + \frac{1}{r}v^1_{0,rr\theta}\right) - \frac{E_3}{1-\nu^2}\left(w^1_{0,rrrr} + \frac{2}{r}w^1_{0,rrr} - \frac{1}{r^2}w^1_{0,rr} + \frac{1}{r^3}w^1_{0,r} + \frac{2}{r^2}w^1_{0,rr\theta\theta} - \frac{2}{r^3}w^1_{0,r\theta\theta} + \frac{4}{r^4}w^1_{0,\theta\theta}\right. \\ &\left. + \frac{1}{r^4}w^1_{0,\theta\theta\theta\theta}\right) + N^0_{rr}w^1_{0,rr} + N^0_{\theta\theta}\left(\frac{1}{r^2}w^1_{0,\theta\theta} + \frac{1}{r}w^1_{0,r}\right) + 2N^0_{r\theta}\left(\frac{1}{r}w^1_{0,r\theta} - \frac{1}{r^2}w^1_{0,\theta}\right) = 0 \end{aligned} \tag{16}$$

With some mathematical manipulations, one may obtain an uncoupled equation in terms of the incremental lateral displacement w_0^1. To this end

1. The first of Eq. (16) is differentiated with respect to r.
2. The first of Eq. (16) is divided by r.
3. The second of Eq. (16) is differentiated with respect to θ and then divided by r.
4. The obtained equations in steps (1)–(3) are added and the result is multiplied by $-\dfrac{E_2}{E_1(1-\nu^2)}$
5. The obtained equation in step (4) is added to the third of Eq. (16).

The resulting equation is an uncoupled equation in terms of w_0^1

$$D_k\left(w^1_{0,rrrr}+\frac{2}{r}w^1_{0,rrr}-\frac{1}{r^2}w^1_{0,rr}+\frac{1}{r^3}w^1_{0,r}+\frac{2}{r^2}w^1_{0,rr\theta\theta}-\frac{2}{r^3}w^1_{0,r\theta\theta}+\frac{4}{r^4}w^1_{0,\theta\theta}+\frac{1}{r^4}w^1_{0,\theta\theta\theta\theta}\right)-N^0_{rr}w^1_{0,rr}-N^0_{\theta\theta}\left(\frac{1}{r^2}w^1_{0,\theta\theta}+\frac{1}{r}w^1_{0,r}\right)-2N^0_{r\theta}\left(\frac{1}{r}w^1_{0,r\theta}-\frac{1}{r^2}w^1_{0,\theta}\right)=0 \tag{17}$$

where $D_k=\dfrac{E_1E_3-E_2^2}{E_1(1-\nu^2)}$ is the equivalent flexural rigidity of an FGM plate. For decoupling of equilibrium or stability equations in polar coordinate based on FSDT one may refer to [7, 20–22, 44]

5 Solving the stability equation

In this section, an exact solution for stability equation (17) is presented. Substituting pre-buckling forces from Eqs. (12) into (17) gives

$$\left(\frac{\partial^2}{\partial r^2}+\frac{1}{r}\frac{\partial}{\partial r}+\frac{1}{r^2}\frac{\partial^2}{\partial\theta^2}\right)\left(\frac{\partial^2}{\partial r^2}+\frac{1}{r}\frac{\partial}{\partial r}+\frac{1}{r^2}\frac{\partial^2}{\partial\theta^2}+\frac{N^T}{D_k}\right)w_0^1(r,\theta)=0 \tag{18}$$

It is more convenient to introduce the following non-dimensional parameters

$$\bar r=\frac{r}{a},\quad \beta=\frac{b}{a},\quad \delta=\frac{h}{a},\mu^2=\frac{N^Ta^2}{D_k} \tag{19}$$

While the in-plane load is symmetric, the buckled shape of the plate may be asymmetric [24, 25, 45, 46]. To this end, the buckling mode of the plate is considered as [47]

$$w_0^1(a\bar r,\theta)=W_n(\bar r)\cos(n\theta) \tag{20}$$

where n is the number of nodal diameters. Here, $n=0$ indicates the symmetric buckled shape of the plate and $n>0$ is associated with the asymmetric buckled shapes. Recalling the definition of non-dimensional parameters (19) and substituting Eqs. (20) into (18), the following ordinary differential equation is obtained

$$\left(\frac{\mathrm{d}^2}{\mathrm{d}\bar r^2}+\frac{1}{\bar r}\frac{\mathrm{d}}{\mathrm{d}\bar r}-\frac{n^2}{\bar r^2}\right)\left(\frac{\mathrm{d}^2}{\mathrm{d}\bar r^2}+\frac{1}{\bar r}\frac{\mathrm{d}}{\mathrm{d}\bar r}-\frac{n^2}{\bar r^2}+\mu^2\right)W_n(\bar r)=0 \tag{21}$$

The exact solution of this equation is obtained as

$$W_n(\bar r)=C_{1n}J_n(\mu\bar r)+C_{2n}Y_n(\mu\bar r)+C_{3n}\bar r^n+C_{4n}\left\{\begin{matrix}\ln\bar r\\ \bar r^{-n}\end{matrix}\right\} \tag{22}$$

Here, $C_{in}, i=1,2,3,4$ are constants to be evaluated when the boundary conditions are applied to Eq. (22). Also J_n and Y_n are the Bessel functions of the first and second kind, respectively. Note that the top form of Eq. (22) is associated with $n=0$ (symmetric buckling) and the bottom one is related to $n>0$ (asymmetric buckling). Equivalently, when the circumferential mode is $n=0$, the function $\ln(\bar r)$ should be used where as when the circumferential mode is $n>0$, the function $\bar r^{-n}$ should be used.

As proved in the previous section, only plates with both inner and outer clamped edges exhibit bifurcation-type buckling for transverse thermal loading. For clamped annular FG plates, boundary conditions are [16]

$$W_n(1)=\frac{\mathrm{d}W_n}{\mathrm{d}\bar r}(1)=W_n(\beta)=\frac{\mathrm{d}W_n}{\mathrm{d}\bar r}(\beta)=0 \tag{23}$$

Recalling Eq. (22), the following system of equations is obtained with the aid of boundary conditions (23)

$$\begin{bmatrix} J_n(\mu) & Y_n(\mu) & 1 & \left\{\begin{matrix}0\\1\end{matrix}\right\}\\ J_n(\mu\beta) & Y_n(\mu\beta) & \beta^n & \left\{\begin{matrix}Ln\beta\\ \beta^{-n}\end{matrix}\right\}\\ [J_n(\mu\bar r)]'_{\bar r=1} & [Y_n(\mu\bar r)]'_{\bar r=1} & n & \left\{\begin{matrix}1\\-n\end{matrix}\right\}\\ [J_n(\mu\bar r)]'_{\bar r=\beta} & [Y_n(\mu\bar r)]'_{\bar r=\beta} & n\beta^{n-1} & \left\{\begin{matrix}\beta^{-1}\\-n\beta^{-n-1}\end{matrix}\right\}\end{bmatrix}\left\{\begin{matrix}C_{1n}\\C_{2n}\\C_{3n}\\C_{4n}\end{matrix}\right\}=\left\{\begin{matrix}0\\0\\0\\0\end{matrix}\right\} \tag{24}$$

To obtain a non-trivial solution, the determinant of the coefficients matrix (24) should set equal to zero. When the determinantal equation is solved, the following explicit expressions are obtained as buckling criteria of the plate

$$\begin{aligned}\frac{4}{\pi\mu}&-\mu\beta\ln\beta(J_1(\mu)Y_1(\mu\beta)-Y_1(\mu)J_1(\mu\beta))\\&+\beta(J_0(\mu)Y_1(\mu\beta)-Y_0(\mu)J_1(\mu\beta))\\&-(J_1(\mu)Y_0(\mu\beta)-Y_1(\mu)J_0(\mu\beta))=0\end{aligned} \tag{25}$$

for $n=0$ (symmetric buckled shape) and

$$\frac{8n}{\pi\mu} - \mu\beta\left(\beta^{n} - \beta^{-n}\right)\left(J_{n+1}(\mu)Y_{n+1}(\mu\beta) - Y_{n+1}(\mu)J_{n+1}(\mu\beta)\right) + 2n\beta^{n+1}\left(J_{n}(\mu)Y_{n+1}(\mu\beta) - Y_{n}(\mu)J_{n+1}(\mu\beta)\right) - 2n\beta^{-n}\left(J_{n+1}(\mu)Y_{n}(\mu\beta) - Y_{n+1}(\mu)J_{n}(\mu\beta)\right) = 0 \tag{26}$$

for $n > 0$ (asymmetric buckled shape).

Now, to obtain the non-dimensional critical buckling loads of the plate, n_{cr}^{T}, for every positive integer number n the associated determinant equation has to be solved. Finding the smallest positive root of the associated equation for each n and choosing the smallest between them yields the associated critical value of μ, which is called μ_{cr}. The non-dimensional critical buckling load of the plate, according to definition (19), is evaluated as $n_{\mathrm{cr}}^{T} = \mu_{\mathrm{cr}}^{2}$.

The temperature distribution through the plate should be known to evaluate the critical buckling temperatures.

6 Types of thermal loading

6.1 Uniform temperature rise

Consider an annular FG plate at reference temperature T_0. When the radial extension is prevented, the uniform temperature may be raised to $T_0 + \Delta T$ such that the plate buckles. Substituting $T = T_0 + \Delta T$ in the fourth of Eq. (8) gives

$$N^{T} = \frac{\Delta T h}{1-\nu}\left(E_m\alpha_m + \frac{E_{cm}\alpha_m + E_m\alpha_{cm}}{k+1} + \frac{E_{cm}\alpha_{cm}}{2k+1}\right) \tag{27}$$

Recalling Eq. (27) and using the definition of n_{cr}^{T} and solving for ΔT, the critical buckling temperature difference of the plate in this case is obtained as

$$\Delta T_{cr} = \frac{\delta^2}{(1+\nu)} \times \frac{e_1 e_3 - e_2^2}{P e_1} n_{\mathrm{cr}}^{T} \tag{28}$$

with

$$P = E_m\alpha_m + \frac{E_m\alpha_{cm} + E_{cm}\alpha_m}{k+1} + \frac{E_{cm}\alpha_{cm}}{2k+1} \tag{29}$$

For an isotropic homogeneous annular plate, ($k = 0$), Eq. (28) reduces to

$$\Delta T_{cr} = \frac{\delta^2}{12(1+\nu)\alpha_c} n_{\mathrm{cr}}^{T} \tag{30}$$

6.2 Linear temperature across the thickness

Consider a thin FGM annular plate where the temperatures at the ceramic-rich and metal-rich surfaces are T_c and T_m, respectively. The temperature distribution for the given boundary conditions is obtained by solving the heat conduction equation along the plate thickness. If the plate thickness is thin enough, the temperature distribution is approximated linear through the thickness. So the temperature as a function of thickness coordinate z can be written in the form

$$T = T_m + (T_c - T_m)\left(\frac{1}{2} + \frac{z}{h}\right) \tag{31}$$

Substituting Eqs. (31) into (8) and solving for $\Delta T = T_c - T_m$ gives the critical buckling temperature difference between the metal-rich and ceramic-rich surfaces as

$$\Delta T_{\mathrm{cr}} = \frac{\delta^2}{(1+\nu)} \times \frac{e_1 e_3 - e_2^2}{Q e_1} n_{\mathrm{cr}}^{T} - (T_m - T_0)\frac{P}{Q} \tag{32}$$

where P is defined by Eq. (29) and Q is equal to

$$Q = \frac{E_m\alpha_m}{2} + \frac{E_m\alpha_{cm} + E_{cm}\alpha_m}{k+2} + \frac{E_{cm}\alpha_{cm}}{2k+2} \tag{33}$$

For an isotropic homogeneous annular plate, ($k = 0$), Eq. (32) reduces to

$$\Delta T_{cr} = \frac{\delta^2}{6(1+\nu)\alpha_c} n_{\mathrm{cr}}^{T} - 2(T_m - T_0) \tag{34}$$

6.3 Non-linear temperature through the thickness

Assume an FGM annular plate where the temperature in ceramic-rich and metal-rich surfaces are T_c and T_m, respectively. The governing equation for the steady-state one-dimensional heat conduction equation, in the absence of heat generation, becomes

$$\frac{\mathrm{d}}{\mathrm{d}z}\left(K(z)\frac{\mathrm{d}T}{\mathrm{d}z}\right) = 0$$

$$T\left(\frac{h}{2}\right) = T_c, \quad T\left(-\frac{h}{2}\right) = T_m \tag{35}$$

Solving this equation via the polynomial series and taking enough terms, yields the temperature distribution across the thickness of the plate. Following the same method used for the linear temperature, the critical bucking temperature difference between the upper and lower surfaces of the plate may be evaluated as

$$\Delta T_{\mathrm{cr}} = \frac{\delta^2}{(1+\nu)} \times \frac{e_1 e_3 - e_2^2}{R e_1} n_{\mathrm{cr}}^{T} - (T_m - T_0)\frac{P}{R} \tag{36}$$

with the following definitions

$$D = \sum_{i=0}^{N} \frac{\left(-\frac{K_{cm}}{K_m}\right)^{i}}{ik+1}$$

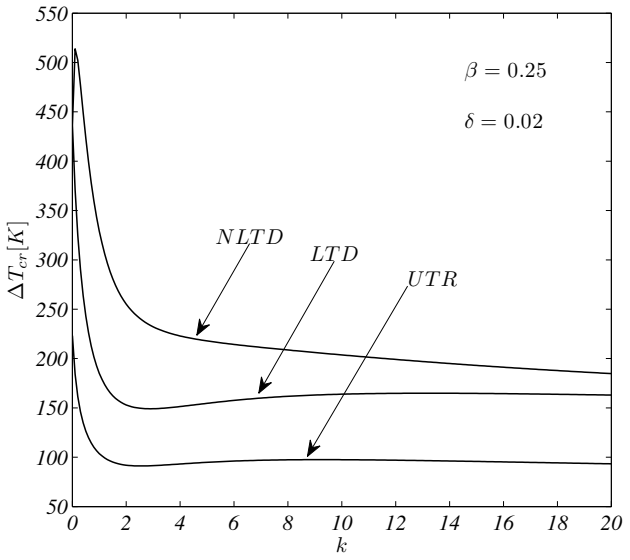

Fig. 2 Influence of the power law index on critical buckling temperature difference $\Delta T_{\rm cr}[K]$ of fully clamped annular FG plates

$$R = \frac{1}{D} \times \left\{ E_m \alpha_m \sum_{i=0}^{N} \frac{(-\frac{K_{cm}}{K_m})^i}{(ik+1)(ik+2)} + (E_{cm}\alpha_m + E_m \alpha_{cm}) \sum_{i=0}^{N} \frac{(-\frac{K_{cm}}{K_m})^i}{(ik+1)(ik+k+2)} + E_{cm}\alpha_{cm} \sum_{i=0}^{N} \frac{(-\frac{K_{cm}}{K_m})^i}{(ik+1)(ik+2k+2)} \right\} \tag{37}$$

where N is the number of sufficient terms to assure the convergence of the series.

For an isotropic homogeneous plate, ($k = 0$), expression (36) simplifies to

$$\Delta T_{\rm cr} = \frac{\delta^2}{6(1+\nu)\alpha_c} n_{\rm cr}^T - 2(T_m - T_0) \tag{38}$$

Table 1 Critical buckling temperature difference $\Delta T_{\rm cr}[K]$ of an isotropic annular plate ($k = 0$) with $\beta = 0.5$ subjected to uniform temperature rise loading

	$\delta = 0.010$	$\delta = 0.015$	$\delta = 0.020$
Present	127.990	287.978	511.960
Li and Cheng [48]	130.693	294.058	522.770
Tani [49]	127.958	287.905	511.831

Table 2 Critical buckling temperature difference $\Delta T_{\rm cr}[K]$ of FG solid circular plates with $a/h = 50$ subjected to non-linear temperature distribution across the thickness

	$k = 0$	$k = 0.5$	$k = 1$
Present	101.590	76.009	61.512
Najafizadeh and Hedayati [50]	101.455	75.915	61.440
Parakash and Ganapathi [51]	101.576	75.913	61.441

Metal-rich surface temperature is kept at reference temperature

which is similar to Eq. (34) because the solution of heat conduction equation (35) is linear across the thickness when thermal conductivity of the plate is position independent.

7 Results and discussions

To illustrate the proposed approach, a ceramic–metal functionally graded annular plate is considered. The combination of materials consists of aluminium and alumina. Material properties are assumed to be temperature independent. This assumption is established to present the critical buckling temperatures in simple closed-form expressions, otherwise, numerical techniques should be implemented to obtain the temperature profile through the plate thickness, iteratively. The elasticity modulus, the thermal expansion coefficient, and the thermal conductivity coefficient for aluminium are $E_m = 70$ GPa, $\alpha_m = 23 \times 10^{-6}$

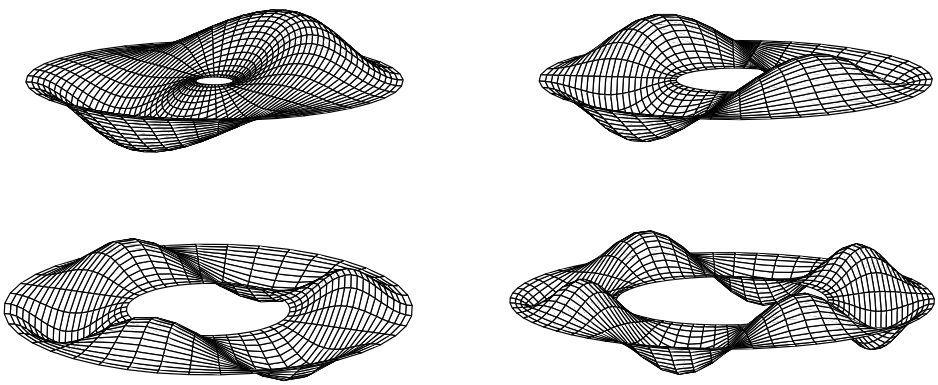

Fig. 3 Buckled configurations of FG plates with various β ratios when $k = 1$. *Left, Up*: $\beta = 0.1$; *Right, Up*: $\beta = 0.2$; *Left, Down*: $\beta = 0.4$; *Right, Down*: $\beta = 0.5$

Table 3 Critical buckling temperature difference $\Delta T_{cr}[K]$ of annular FG plates subjected to uniform temperature rise loading for various β and δ ratios

β	δ	$k=0$	$k=0.5$	$k=1$	$k=2$	$k=5$	$k=\infty$
	0.010	33.711	19.100	15.661	13.884	14.324	10.846
$0.05^{n=1}$	0.015	75.849	42.974	35.237	31.240	32.230	24.404
	0.020	134.843	76.398	62.644	55.538	57.297	43.384
	0.010	39.002	22.098	18.119	16.064	16.573	12.549
$0.10^{n=1}$	0.015	87.755	49.720	40.768	36.144	37.288	28.234
	0.020	156.009	88.390	72.478	64.255	66.291	50.194
	0.010	43.227	24.491	20.082	17.804	18.368	13.908
$0.15^{n=2}$	0.015	97.261	55.105	45.185	40.059	41.238	31.239
	0.020	172.908	97.965	80.238	71.216	73.472	55.631
	0.010	48.758	27.625	22.651	20.082	20.718	15.687
$0.20^{n=2}$	0.015	109.707	62.157	50.967	45.185	46.616	35.297
	0.020	195.034	110.501	90.607	80.328	82.873	62.750
	0.010	55.791	31.610	25.919	22.979	23.707	17.950
$0.25^{n=2}$	0.015	125.530	71.122	58.318	51.702	53.340	40.388
	0.020	223.164	126.439	103.676	91.914	94.827	71.800
	0.010	64.619	36.611	30.020	26.614	27.458	20.790
$0.30^{n=2}$	0.015	145.392	82.375	67.545	59.882	61.780	46.778
	0.020	258.474	146.445	120.080	106.458	109.830	83.161
	0.010	75.620	42.844	35.131	31.146	32.132	24.330
$0.35^{n=3}$	0.015	170.145	96.400	79.045	70.017	72.298	54.742
	0.020	302.480	171.377	140.524	124.582	128.529	97.320
	0.010	88.357	50.061	41.048	36.391	37.545	28.428
$0.40^{n=3}$	0.015	198.804	112.637	92.359	81.881	84.475	63.963
	0.020	353.430	200.244	164.194	145.567	150.178	113.712
	0.010	105.423	59.730	48.976	43.420	44.796	33.919
$0.45^{n=3}$	0.015	237.201	134.392	110.197	97.696	100.791	76.317
	0.020	421.691	238.919	195.906	173.681	179.184	135.674
	0.010	127.990	72.516	59.461	52.715	54.385	41.179
$0.50^{n=4}$	0.015	287.978	163.160	133.783	118.609	122.367	92.654
	0.020	511.960	290.063	237.842	210.861	217.541	164.718
	0.010	157.954	89.492	73.381	65.056	67.117	50.820
$0.55^{n=4}$	0.015	355.396	201.358	165.107	146.377	151.014	114.345
	0.020	631.615	357.970	293.524	260.225	268.470	203.280
	0.010	200.147	113.398	92.983	82.435	85.046	64.395
$0.60^{n=5}$	0.015	450.332	255.146	209.212	185.478	191.354	144.889
	0.020	800.859	453.593	371.932	329.738	340.185	257.581

/K and $K_m = 204$ W/mK, and for alumina are $E_c = 380$ GPa, $\alpha_c = 7.4 \times 10^{-6}$/K and $K_c = 10.4$ W/mK, respectively. For simplicity, Poisson's ratio is chosen to be 0.3 [14]. The plate is assumed to be clamped at both inner and outer edges.

In Table 1, to show the validity and accuracy of the present method, the critical buckling temperature difference of thin annular isotropic plates is compared with those reported in [23] based on the numerical shooting method and results of Tani [49]. As seen, a small difference between our result and those reported in [23] is observed which is due to neglecting the asymmetrical deformation of annular plates under symmetrical in-plane loading in [23]. As seen, the comparison is well justified.

In another comparison study, critical buckling temperatures of solid circular plates for nonuniform thermal loading are provided. Comparison is provided in Table 2. The temperature profile through the thickness is obtained according to non-linear temperature distribution obtained from the heat conduction equation. A solid circular plate with radius to thickness ratio $a/h = 50$ is considered. Inner radius is set equal to zero. Boundary conditions on the inner edge of the plate is considered to be sliding support. It is seen that numerical results of this study match

well with the results of Najafizadeh and Hedayati [50] and Prakash and Ganapathi [51].

The influence of power law index on critical buckling temperature difference of annular FG plates is depicted in Fig. 2. Geometrical parameters are chosen as $\beta = 0.25$ and $\delta = 0.02$. A $5K$ increase in metal-rich surface of the plate is considered, i.e. $T_m - T_0 = 5K$. As seen, when the power law index of FG plates becomes larger, curves behaviour in each case of thermal loading is different. When plate is subjected to uniform temperature rise (UTR), and power law index increases up to 2, $\Delta T_{\rm cr}$ inherits a swift descend, while for $2 < k < 10$ the value of $\Delta T_{\rm cr}$ increases very slow, and finally non-significant decrease occurs for $k > 10$. For non-linear temperature across the thickness (NLTD), $\Delta T_{\rm cr}$ increases up for initial values of power law index and then decreases permanently. In comparison with rapid changes in $\Delta T_{\rm cr}$ for $k < 2$, alternations for $k > 2$ are not significant. It should be pointed out that the linear temperature distribution across the thickness (LTD), which is an approximation for exact heat conduction equation (35), underestimates the critical buckling temperatures, except for $k = 0$ and $k = \infty$, when FGM annular plate reduces to a full-metal or full-ceramic plate. In these cases, the exact solution of heat conduction equation is also linear.

Buckled configurations of clamped annular FG plates ($k = 1$) for some β ratios are depicted in Fig. 3. As seen for all cases, ($\beta = 0.1, 0.3, 0.4, 0.5$) plates buckle in asymmetric modes. The associated buckling modes are $n = 1, 2, 3, 4$, respectively. As seen, by increasing the β ratio, number of nodal diameters increases.

Table 3 presents the buckling temperature difference of thin FG annular plate subjected to UTR case for various power law index, β and δ ratios. As expected, when plate becomes thicker the buckling temperatures become higher, which is due to an increase in the flexural rigidity of the plate. As seen, the critical buckling temperature becomes higher when the ratio β increases. It should be noted that the number of nodal points for each β are indicated as superscripts. As seen for all cases, asymmetric buckling configuration occurs, i.e. $n > 0$. Furthermore, the critical buckling temperature of non-homogeneous plate ($0 < k < \infty$) lies between the associated values of plates made of ceramic and metal constituents, respectively.

The influence of δ and β ratios on bifurcation buckling of FG plates for linear and non-linear cases of temperature distribution is depicted in Figs. 4 and 5, respectively. The linear composition of ceramic–metal is assumed for the FG annular plates. As expected, when δ increases the critical buckling temperature of FG plates becomes higher due to an increase in the flexural rigidity of the plate. Also as β diminishes, $\Delta T_{\rm cr}$ decreases permanently.

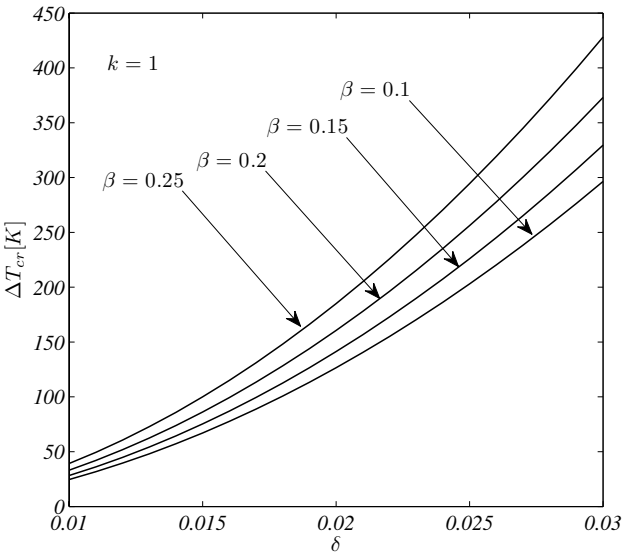

Fig. 4 Influence of thickness and inner radius on critical buckling temperature difference of annular FG plates subjected to linear temperature distribution across the thickness

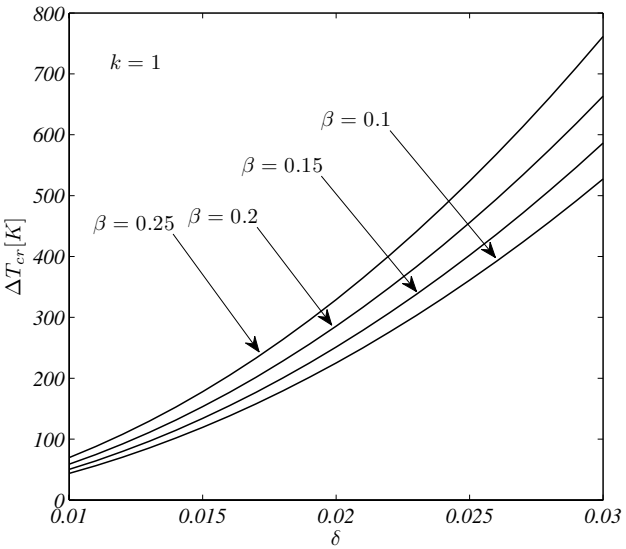

Fig. 5 Influence of thickness and inner radius on critical buckling temperature difference of annular FG plates subjected to heat conduction across the thickness

To obtain a clear understanding on hoop mode alternation with respect to β ratio, Table 4 presents the range of the β ratio for a specified number of nodal diameters. As one may obtain, in the range $0.001 < \beta < 1$, piecewise increase in number of nodal diameters is observed with respect to the permanent increase of β ratio. At higher values of β, number of nodal diameters changes rapidly.

Table 4 Range of β ratio to obtain a certain number of nodal diameters indicated as superscripts

$(0.001-0.101)^{1}$	$(0.102-0.346)^{2}$	$(0.347-0.487)^{3}$	$(0.488-0.577)^{4}$	$(0.578-0.641)^{5}$
$(0.642-0.687)^{6}$	$(0.688-0.723)^{7}$	$(0.724-0.752)^{8}$	$(0.753-0.775)^{9}$	$(0.776-0.794)^{10}$
$(0.795-0.810)^{11}$	$(0.811-0.824)^{12}$	$(0.825-0.836)^{13}$	$(0.837-0.847)^{14}$	$(0.848-0.856)^{15}$
$(0.857-0.864)^{16}$	$(0.865-0.871)^{17}$	$(0.872-0.878)^{18}$	$(0.879-0.884)^{19}$	$(0.885-0.889)^{20}$

8 Conclusion

In the present article the equilibrium and stability equations for a thin annular heated FG plates are obtained. The derivation is based on the classical plate theory, while the constituent materials follow the power law form of property distribution. The boundary conditions of plate on both edges are assumed to be hard clamped. Closed-form solutions are derived for the critical buckling temperatures. It is concluded that

1. In general, bifurcation-type buckling does not exist for annular FG plates. Boundary conditions on both inner and outer edges have a great effect on dictating the behaviour of the plate under in-plane thermal loading. Only fully clamped annular FG plates exhibit bifurcation-type buckling, where for other combinations of boundary conditions plate exhibit a non-linear bending with the presence of thermal loading.
2. While the temperature distribution is symmetric through the plate, buckled configurations of clamped-clamped FG plates are all asymmetric.
3. The number of nodal diameters and critical buckling temperatures of FG plates increase when β ratio gets larger.
4. The number of nodal diameters of FG plates and isotropic homogeneous plates are similar to each other when the geometric parameters are kept constant.

References

1. Nie G, Zhong Z (2007) Axisymmetric bending of two-directional functionally graded circular and annular plates. Acta Mech Solida Sin 20(4):289–295
2. Nie G, Zhong Z (2010) Dynamic analysis of multi-directional functionally graded annular plates. Appl Math Model 34(3):608–618
3. Noseir A, Fallah F (2009) Non-linear analysis of functionally graded circular plates under asymmetric transverse loading. Int J Nonlinear Mech 44(8):928–942
4. Reddy JN, Wang CM, Kitipornchai S (1999) Axisymmetric bending of functionally graded circular and annular plates. Eur J Mech A Solids 18(2):185–199
5. Saidi AR, Rasouli A, Sahraee S (2009) Axisymmetric bending and buckling analysis of thick functionally graded circular plates using unconstrained third-order shear deformation plate theory. Compos Struct 89(1):110–119
6. Sahraee S, Saidi A (2009) Axisymmetric bending analysis of thick functionally graded circular plates using fourth-order shear deformation theory. Eur J Mech A Solids 28(5):974–984
7. Nosier A, Fallah F (2008) Reformulation of Mindlin-Reissner governing equations of functionally graded circular plates. Acta Mech 198(3–4):209–233
8. Hosseini-Hashemi Sh, Fadaee M, Eshaghi M (2010) A novel approach for in-plane/out-of-plane frequency analysis of functionally graded circular/annular plates. Int J Mech Sci 52(8):1025–1035
9. Dong CY (2009) Three-dimensional free vibration analysis of functionally graded annular plates using the Chebyshev-Ritz method. Mater Des 29(8):1518–1525
10. Aghdam MM, Shahmansouri N, Mohammadi M (2012) Extended Kantorovich method for static analysis of moderately thick functionally graded sector plates. Math Comput Simul 29(1):118–130
11. Tajeddini V, Ohadi A, Sadighi M (2011) Three-dimensional free vibration of variable thickness thick circular and annular isotropic and functionally graded plates on Pasternak foundation. Int J Mech Sci 53(4):300–308
12. Afsar AM, Go J (2010) Finite element analysis of thermoelastic field in a rotating FGM circular disk. Appl Math Model 34(11):3309–3320
13. Najafizadeh MM, Eslami MR (2002) Buckling analysis of circular plates of functionally graded materials under uniform radial compression. Int J Mech Sci 44(12):2479–2493
14. Najafizadeh MM, Eslami MR (2002) First-order-theory-based thermoelastic stability of functionally graded material circular plates. AIAA J 40(7):1444–1450
15. Najafizadeh MM, Heydari HR (2008) An exact solution for buckling of functionally graded circular plates based on higher order shear deformation plate theory under uniform radial compression. Int J Mech Sci 50(3):603–612
16. Najafizadeh MM, Heydari HR (2004) Thermal buckling of functionally graded circular plates based on higher order shear deformation plate theory. Eur J Mech A Solids 23(6):1085–1100
17. Jalali SK, Naei MH, Poorsolhjouy A (2010) Thermal stability analysis of circular functionally graded sandwich plates of variable thickness using pseudo-spectral method. Mater Des 31(10):4755–4763
18. Ma LS, Wang TJ (2003) Nonlinear bending and post-buckling of a functionally graded circular plate under mechanical and thermal loadings. Int J Solids Struct 40(13–14):3311–3330
19. Kiani Y, Eslami MR (2015) Thermal post-buckling of imperfect circular functionally graded material plates : examination of Voight, Mori-Tanaka and self-consistent Schemes. J Pres Vessel Technol 137(2):Article number: 021201
20. Naderi A, Saidi AR (2011) An analytical solution for buckling of moderately thick functionally graded sector and annular sector plates. Arch Appl Mech 81(6):801–828
21. Saidi AR, Hasani Baferani A (2010) Thermal buckling analysis of moderately thick functionally graded annular sector plates. Compos Struct 92(7):1744–1752
22. Naderi A, Saidi AR (2011) Exact solution for stability analysis of moderately thick functionally graded sector plates on elastic foundation. Compos Struct 93(2):629–638
23. Li SR, Zhang JH, Zhao YG (2007) Nonlinear thermomechanical post-buckling of circular FGM plate with geometric imperfection. Thin Wall Struct 45(5):528–536

24. Kiani Y, Eslami MR (2013) An exact solution for thermal buckling of annular plate on an elastic medium. Compos Part B Eng 45(1):101–110
25. Kiani Y, Eslami MR (2013) Instability of heated circular FGM plates on a partial Winkler-type foundation. Acta Mech 224(5):1045–1060
26. Sepahi O, Forouzan MR, Malekzadeh P (2011) Thermal buckling and postbuckling analysis of functionally graded annular plates with temperature-dependent material properties. Mater Des 32(7):4030–4041
27. Aghelinejad M, Zare K, Ebrahimi F, Rastgoo A (2011) Nonlinear thermomechanical post-buckling analysis of thin functionally graded annular plates based on von-Karman's plate theory. Mech Adv Mater Struct 18(5):319–326
28. Shen HS, Wang ZX (2012) Assessment of Voigt and Mori-Tanaka models for the vibration analysis of functionally graded plates. Compos Struct 94(7):2197–2208
29. Hetnarski RB, Eslami MR (2009) Thermal stresses advanced theory and applications. Springer, Berlin
30. Esfahani SE, Kiani Y, Eslami MR (2013) Non-linear thermal stability analysis of temperature dependent fgm beams supported on non-linear hardening elastic foundations. Int J Mech Sci 69:10–20
31. Komijani M, Kiani Y, Esfahani SE, Eslami MR (2012) Vibration of thermo-electrically post-buckled rectangular functionally graded piezoelectric beams. Compos Struct 98:143–152
32. Kiani Y, Eslami MR (2010) Thermal buckling analysis of functionally graded material beams. Int J Mech Mater Des 6(3):229–238
33. Kiani Y, Rezaei M, Taheri S, Eslami MR (2011) Thermo-electrical buckling of piezoelectric functionally graded material Timoshenko beams. Int J Mech Mater Des 7(3):185–197
34. Kiani Y, Taheri S, Eslami MR (2011) Thermal buckling of piezoelectric functionally graded material beams. J Therm Stress 34(8):835–850
35. Kiani Y, Eslami MR (2013) Thermomechanical buckling of temperature-dependent FGM beams. Lat Am J Solids Struct 10(2):223–246
36. Asadi H, Kiani Y, Shakeri M, Eslami MR (2014) Exact solution for nonlinear thermal stability of hybrid laminated composite Timoshenko beams reinforced with SMA fibers. Compos Struct 108:811–822
37. Esfahani SE, Kiani Y, Komijani M, Eslami MR (2013) Vibration of a temperature-dependent thermally pre/postbuckled FGM beam over a nonlinear hardening elastic foundation. J Appl Mech 81(1):JAM-12-1467
38. Bateni M, Kiani Y, Eslami MR (2014) A comprehensive study on stability of FGM plates. Int J Mech Sci 75:134–144
39. Kargani A, Kiani Y, Eslami MR (2011) Exact solution for nonlinear stability of piezoelectric FGM Timoshenko beams under thermo-electrical loads. J Therm Stress 36(10):1056–1076
40. Ghiasian SE, Kiani Y, Eslami MR (2014) Thermal buckling of shear deformable temperature dependent circular/annular FGM plates. Int J Mech Sci 81:137–148
41. Kiani Y, Eslami MR (2013) Nonlinear thermo-inertial stability of thin circular FGM plates. J Frankl Inst 351(2):1057–1073
42. Mirzaei M, Kiani Y (2016) Thermal buckling of temperature dependent FG-CNT reinforced composite plates. Meccanica. doi:10.1007/s11012-015-0348-0
43. Asadi H, Kiani Y, Shakeri M, Eslami MR (2014) Exact solution for nonlinear thermal stability of geometrically imperfect hybrid laminated composite Timoshenko beams embedded with SMA fibers. J Eng Mech 141(4):14. Article Number: 04014144
44. Saidi AR, Hejripour F, Jomehzadeh E (2010) On the stress singularities and boundary layer in moderately thick functionally graded sectorial plates. Appl Math Model 34(11):3478–3492
45. Yamaki N (1958) Buckling of a thin annular plate under uniform compression. J Appl Mech 25(11):267–273
46. Wang CM, Wang CY, Reddy JN (2004) Exact solutions for buckling of structural members. CRC Press, Boca Raton
47. Wang CY, Aung TM (2005) Buckling of circular Mindlin plates with an internal ring support and elastically restrained edge. J Eng Mech 131(4):359–366
48. Li SR, Cheng CJ (1991) Thermal buckling of thin annular plates under multiple loads. Appl Math Mech Engl Ed 12(3):301–308
49. Tani J (1981) Elastic instability of a heated annular plate under lateral pressure. J Appl Mech 48(2):399–403
50. Najafizadeh MM, Hedayati B (2004) Refined theory for thermoelastic stability of functionally graded circular plates. J Therm Stress 27(9):857–880
51. Prakash T, Ganapathi M (2006) Asymmetric flexural vibration and thermoelastic stability of FGM circular plates using finite element method. Compos Part B Eng 37(7–8):642–649